PHYSICS AND CHEMISTRY OF SOLID STATE
V. 26, No. 2 (2025) pp. 251-260
Section: Technology

DOI: 10.15330/pcss.26.2.251-260

Vasyl Stefanyk Precarpathian National University

ФІЗИКА І ХІМІЯ ТВЕРДОГО ТІЛА
Т. 26, № 2 (2025) С. 251-260
Технічні науки

PACS: 61.43.Gt, 81.05.Uw, 84.37.+q

ISSN 1729-4428 (Print)
ISSN 2309-8589 (Online)

V.I. Mandzyuk[1], N.I. Nagirna[2], R.V. Solomovskyi[1], N.A. Ostapyshyn[1]

Impedance spectrocopy of carbonized and thermal activated porous carbon materials

[1]Vasyl Stefanyk Precarpathian National University, Ivano-Frankivsk, Ukraine, volodymyr.mandzyuk@pnu.edu.ua
[2]Separate Structural Subdivision "Professional College of Electronic Devices Ivano-Frankivsk National Technical University of Oil and Gas", Ivano-Frankivsk, Ukraine

Using the impedance spectroscopy method, a comparative analysis of the kinetics of the electrochemical insertion of lithium ions into a porous carbon material obtained by hydrothermal carbonization of plant raw materials at a temperature of 750°C (PCM-C sample) and its subsequent thermal activation at a temperature of 400°C for 2.5 h (PCM-TA sample) was carried out. For electrochemical systems based on these materials, equivalent electrical circuits were selected that satisfactorily model the impedance spectra in the studied frequency range of 10^{-2} -10^{5} Hz. A physical interpretation was proposed for each element of the circuit. The diffusion coefficient of lithium ions into the structure of electrode materials was calculated.

Keywords: porous carbon material, carbonization, thermal activation, electrochemical insertion, impedance spectroscopy, equivalent electric circuit, diffusion coefficient.

Received 14 January 2024; Accepted 15 May 2025.

Introduction

In recent decades, porous carbon materials (PCMs) of micro- and nanometric sizes due to their specific surface area, electrochemical stability, high electrical conductivity and low cost have found wide application as electrode materials in lithium power sources [1-6]. The electrochemical insertion of lithium ions into PCMs is accompanied by various processes, such as diffusion into the electrolyte solution, migration through the surface film, charge transfer at the carbon/electrolyte interface and diffusion inside the carbon electrode. Various experimental methods are used to study these processes, such as potentiostatic intermittent titration technique [7], intermittent current interruption [8], current pulse relaxation method [9], cyclic voltamperometry [10], galvanostatic intermittent titration technique [11], electrochemical impedance spectroscopy [12]. The latter method deserves special attention, as it allows for research in a fairly wide frequency range ($f = 10^{6}$ - 10^{-3} Hz) and is based on a systems approach, according to which the object under study is considered as an equivalent electrical circuit (EEC), containing elements that characterize both the electrode/electrolyte phase boundary and the properties of the solid.

The aim of this work is a comparative analysis of processes in electrochemical systems based on carbonized and thermally activated porous carbon materials using the impedance spectroscopy method, which, according to previous studies, have a maximum specific capacity of 1355 [13] and 1511 mA·h/g [14], respectively, as active electrode materials of lithium power sources.

I. Materials and methods

PCMs obtained by hydrothermal carbonization of plant raw materials at a temperature of 750°C (PCM-C sample) and its subsequent thermal activation at a temperature of 400°C for 2.5 h (PCM-TA sample) were selected for the investigation.

The starting material for carbonization was apricot kernels, mechanically crushed, which were placed in an autoclave with distilled water. The autoclave was placed in an oven, where the initial PCM-C was obtained for 1 h

at a constant temperature. The material obtained after the carbonization process was subjected to mechanical grinding twice.

For thermal activation, the PCM-C initial material was placed in a special chamber, where it was kept for a specified time and temperature in a gas flow-mixture of hot air and argon. The gas mixture was supplied using a gas supply system, which was modified according to the type of reacting gas. The gases were cleaned of resinous impurities and directed to the exhaust system.

The cathodes of electrochemical cells were made from a homogeneous mixture of PCM and a binding component (teflon) in a mass ratio of 96% : 4%, respectively. Acetone was added to the mixture to obtain a pasty consistency, which was applied to a nickel grid of 5×5 mm in size. The reference electrode was made from lithium foil by pressing it onto a nickel grid. The electrodes were immersed in an electrolyte solution, after which the cell was sealed. A one-molar solution of lithium tetrafluoroborate salt $LiBF_4$ in γ-butyrolactone was used as an electrolyte. Electrochemical cells were made in a glove box dried by P_2O_5 and filled with argon. The equilibrium electrode potential of the PCMs relative to the lithium reference electrode was 3.2 – 3.4 V.

The electrochemical reaction of lithium ion insertion into the PCMs is described by the equation

$$C + xLi^+ + xe^- \rightarrow Li_xC, \quad (1)$$

where x is the degree of lithium ioninsertion, which is determined based on the ratio:

$$x = \frac{M\,I\,t}{n\,F\,m}, \quad (2)$$

where n is the number of reaction electrons, M and m are the molar mass and mass of the PCM, respectively, F is the Faraday constant, I is the discharge current, t is the discharge time.

Impedance investigates were carried out using an Autolab amplitude-frequency analyzer (Netherlands) in the range of 10^{-2} - 10^5 Hz. The parameters of the EEC elements were found by minimizing the root mean square deviation of the measured impedance modulus from the impedance modulus calculated for the proposed EEC using the ZView-2 computer software.

II. Results and discussion

The kinetics of the electrochemical insertion of lithium ions into the PCMs will determine both the form of the impedance spectrum and the choice of the EEC acceptable for a specific degree of insertion x [15].

According to impedance spectroscopy data for the PCM-C sample, the Nyquist diagram has the form of a straight line in the high-frequency region of the spectrum and passes at an angle of about 45° to the real axis Z' (Fig. 1). This high-frequency arc is associated with the difficult mass transfer in the solid electrolyte interface (SEI), which has lithium-cation conductivity [16]. Passing this layer by lithium ions occurs by the diffusion mechanism. The mid-frequency region of the spectrum has the form of a deformed semicircle, the radius of which increases with increasing x. This semicircle is due to the difficult charge transfer through the electrode / electrolyte interface. For all x-values in the low-frequency range, there is a linear region in the spectrum, which is characterized by a different angle of inclination to the real axis and changes from a "quasi-vertical" (capacitive) line to a diffusion line (angle of inclination is about 45°) with increasing x. This region of the spectrum is identified with the accumulation of electric charge in the volume of the electrode material and the slowed diffusion of "guest" particles into the "host" material.

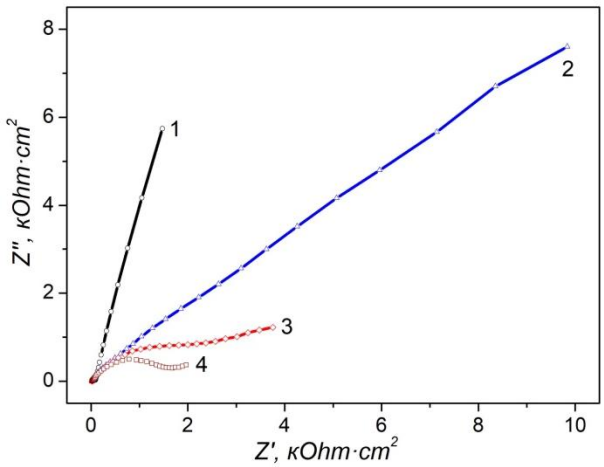

Fig. 1. Nyquist diagrams of the electrochemical system based on the PCM-C sample at different degrees of insetrion: $x = 0.025$ (curve 1); $x = 0.078$ (curve 2); $x = 0.112$ (curve 3); $x =$ (curve 4).

As follows from these diagrams the process of electrochemical insertion of lithium ions into PCM-C can be divided into 4 stages.

The first stage at $0 < x < 0.078$ describes the accumulation (adsorption) of lithium ions on the PCM-C surface, which is accompanied by the decomposition of the electrolyte and the beginning of the SEI formation. According to [17] the SEI film is formed by carbonates, fluorides and lithium oxide-hydroxides. These processes are the result of side electrochemical reactions occurring at the electrode / electrolyte interface. In the second and third stages, the entire surface of the PCM is covered with SEI ($0.078 \leq x < 0.141$). In parallel, this layer grows in thickness and transforms until the electrochemical cell is completely discharged. When $x > 0.141$, along with the processes on the surface, the formation of Li_xC phases occurs due to the lithium ion insertion into PCM-C (stage 4).

The qualitative analysis of the change in impedance spectra with increasing of insertion degree allowed to select the EECs that give the real passing of electrochemical processes in the studied system. The application of the proposed EECs at all values of x allowed to approximate the experimental spectrum to the calculated one with acceptable accuracy. In particular, the Kramers-Cronig coefficient did not exceed $5 \cdot 10^{-4}$ and the difference between the experimental and model curves was 10%.

To model electrochemical processes occurring at stage 1, an EEC was proposed (Fig. 2, a), in which the R_{el}

element is the electrolyte resistance, the $CPE_1 \parallel R_1$ link characterizes the process of charge transfer across the electrolyte / SEI interface, the $C_2 \parallel R_2$ link characterizes the process of charge transfer across the electrolyte / PCM-C interface (the C_2 element is the capacitance of the double electric layer (DEL) formed by lithium ions at this interface, R_2 is the charge transfer resistance across this interface). In the low-frequency range, the impedance spectrum is modeled by sequentially including the intercalation capacitance CPE_{int} in the circuit. According to the results of calculations of the EEC element parameters, the CPE_1 element is a diffusion-type element, and the CPE_{int} is a capacitive one. This is confirmed by the value of the CPE_P parameter, which is close to 0.5 for the first element and 0.9 for the second.

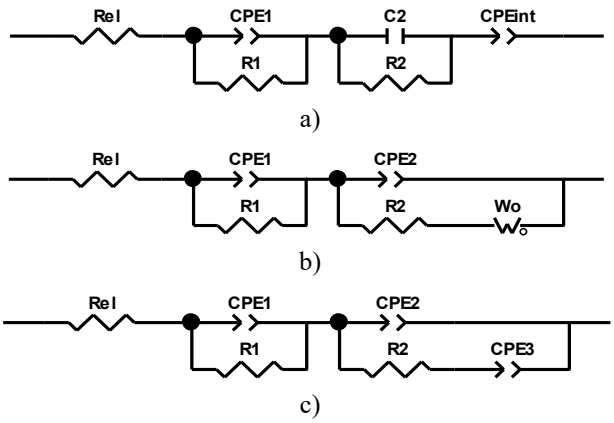

Fig. 2. EECs, which represents the process of electrochemical insetrion of lithium ions into PCM-C.

Increasing the x value causes a change in the shape of the Nyquist diagrams, which, in turn, leads to a change in the EEC. Under the condition of $x = 0.078$, when the entire surface of the PCM is covered with SEI film, the C_2 element is replaced by the CPE_2 constant phase element, and the C_{int} element is replaced by the W_o element. These elements describe the diffusion process of charge transfer across the SEI-PCM interface and in the electrode material, respectively (Fig. 2, b). The scheme, which was called the generalized Randles-Erschler model [15], was also used to simulate impedance spectra at $0.078 < x < 0.141$. When $x > 0.141$, the Warburg impedance in this scheme is replaced by a diffusion-type constant phase element (Fig. 2, c).

When $x \geq 0.078$ the entire surface of the PCM-C is covered with a SEI film. In this case, the charge is transferred through the electrolyte-SEI interface, SEI and the SEI-PCM interface. The indicated processes should be represented in the EEC by including three series-connected $R \parallel C$ (or $R \parallel CPE$) links (Voigt model [15]). However, these processes are not frequency-separated, are characterized by different, but close time constants $\tau = R \cdot C$. Therefore, there are no three semi-circles clearly separated from each other on the Nyquist diagram. In order to avoid ambiguities in the interpretation of the modeling results, only one $R_1 \parallel CPE_1$-link was used (Fig. 2, b, c), in which the resistance R_1 is the sum of the resistances of all interfaces $R_1 = R' + R'' + R'''$, the CPE_1 element is their capacitance (according to the simulation, when x changes from 0.078 to 0.435, the CPE_{1P} parameter is in the range 1 - 0.8, which indicates its capacitive behavior).

Taking into account the correctness of the selection of the EECs and the correspondence of the circuit elements to real physical processes, the evolution of the EEC elements over time when the equilibrium electrode potential changes in the electrochemical system based on the PCM-C sample was investigated.

The formation of a SEI film on the carbon particle surface and its growth causes a monotonic nonlinear increase in the resistance R_1 due to an increase in its geometric sizes. The decrease of the CPE_1 parameter is due to both an increase in the SEI thickness and the gradual blocking of the material surface by the SEI film, which, in turn, makes it difficult to deliver lithium ions to its surface (Fig. 3, a).

The parameters responsible for the charge transfer process across the electrolyte-PCM interface will also undergo changes (Fig. 3, b). A decrease in the contact area of the electrolyte with carbon due to the SEI formation leads to a decrease in the DEL capacitance C_2, and the insertion of the "first" lithium ions into the carbon particles creates an electrostatic barrier when introducing subsequent ions, as a result the resistance R_2 increases sharply. The decrease in the intercalation pseudocapacitance CPE_{int} is due to the fact that an increasing part of the lithium ions inserted into the PCM-C participate in the SEI formation, thereby reducing its content in the surface layers of the carbon particles (Fig. 3, c). After the completion of the first stage of the lithium ion insertion into the PCM-C (EEC in Fig. 2, a), the entire surface of the electrode material is covered with SEI film.

The next task is to find out how the parameters of the EEC elements (Fig. 2, b, c) change with a further increase in the insertion degree x. The element CPE_1, which at $x \geq 0.078$ is a capacitive type element, monotonically decreases (Fig. 4, a), which is represented by the dependence $C = \frac{\varepsilon\varepsilon_0 S}{d}$ (S, d and ε are the area, thickness and dielectric constant of the SEI film, respectively, ε_0 is the electric constant). Among these quantities, the SEI thickness changes the most with increasing x, while its area and dielectric constant remain unchanged. The slight deviation of this parameter from the dependence $CPE_1 = f(\frac{1}{d})$ is most likely due to the processes occurring during the SEI formation, i.e. its local destruction and subsequent "healing". These processes will also affect the value of the element R_1, which represents the resistance of this layer (Fig. 4, a). It follows from the figure that an increase in the SEI thickness causes an increase in its resistance R_1, which is described by the equality $R = \frac{\rho d}{S}$ (ρ is the SEI resistivity). When $x > 0.13$, the resistance R_1 almost does not change, which indicates the stabilization of the structure and properties of this layer.

More difficult to explain is the behavior of the dependence $CPE_2 = f(x)$ (Fig. 4, b). As noted above, this element is responsible for the diffusion process of charge transfer across the SEI-PCM interface. When $x \leq 0.13$, the SEI thickness increases, resulting in an increase in the charge transfer resistance. Changes in the electrode material volume due to the lithium ion insertion into the

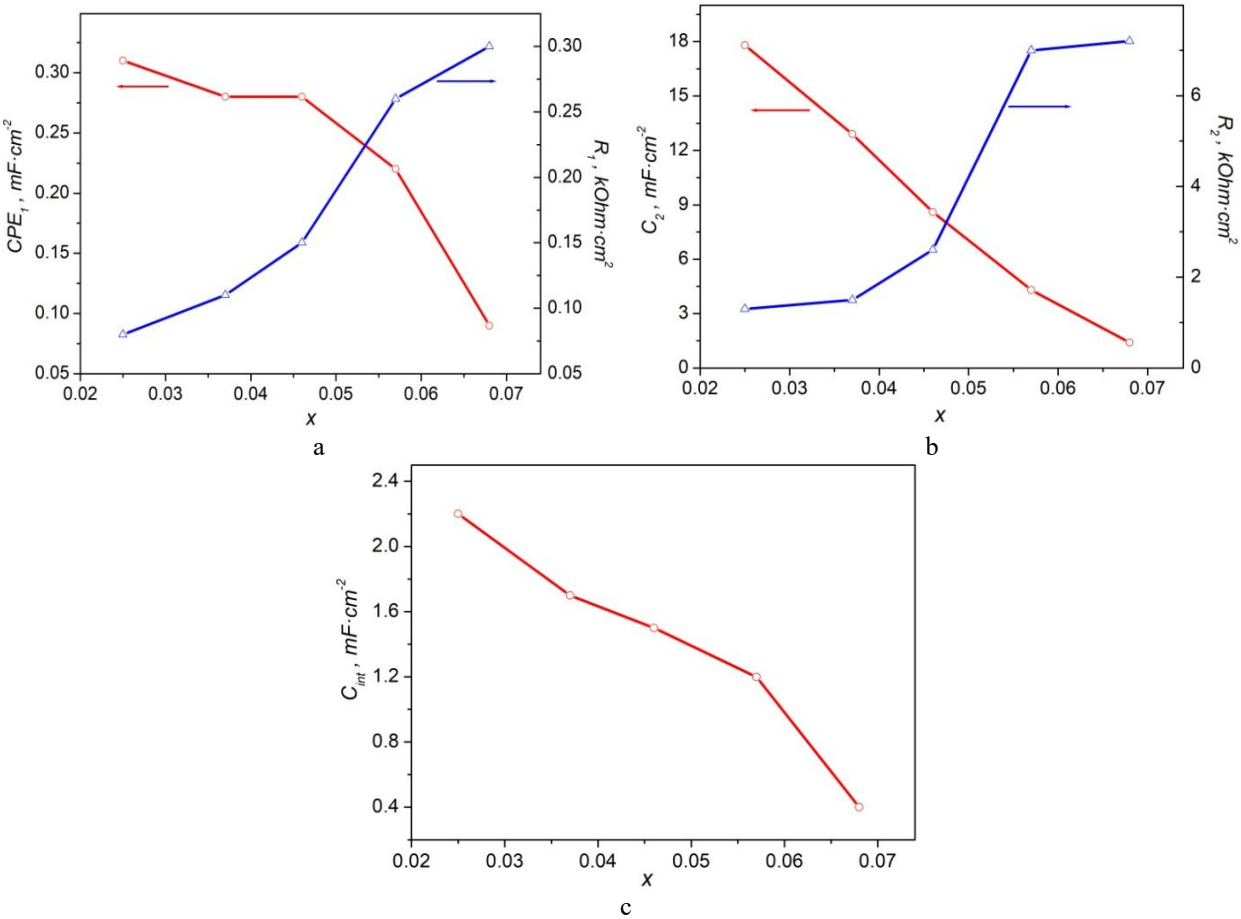

Fig. 3. The change in EEC parameters at the first stage of lithium ion insertion into PCM-C.

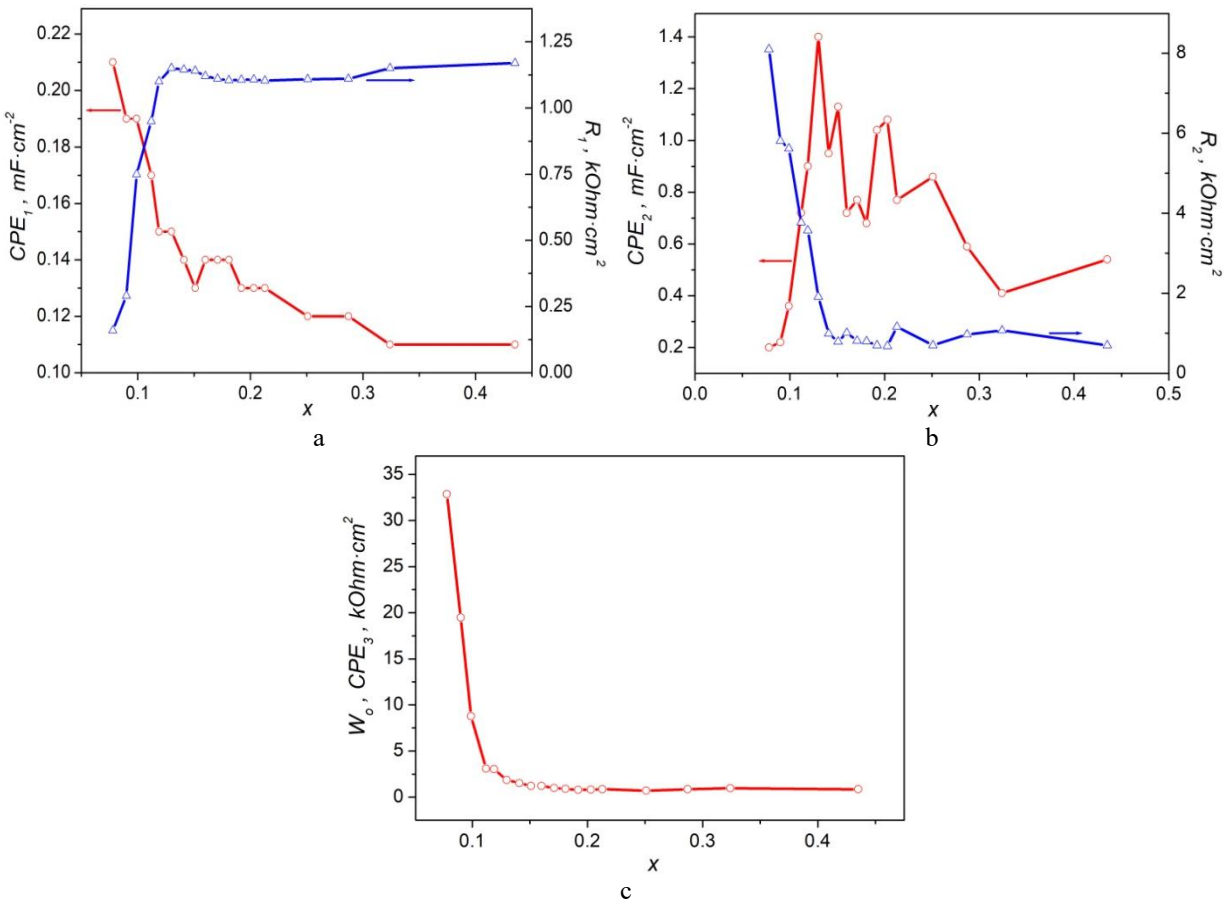

Fig. 4. The change in EEC parameters at the second and third stages of lithium ions insertion into PCM-C.

PCM particles lead to partial SEI destruction and, as a result, fluctuations in the CPE_2 parameter when x increases. The value of the element R_2, which represents the charge transfer resistance in the PCM particles, due to the formation of conduction channels in the active material in particular and the increase in the electronic component of the conductivity of the electrode material in general, sharply decreases when $x \approx 0.141$, and then practically does not change, which indicates the stabilization of the process of lithium ion insertion into the PCM-C structure due to the formation of a continuous series of non-stoichiometric phases of insertion Li_xC (Fig. 4, b). This result is also confirmed by the change in the parameter W (or CPE_3), which is responsible for the diffusion limitations on charge transfer in the PCM particles (Fig. 4, c).

Based on impedance spectroscopy data, the coefficient of electrically stimulated diffusion of lithium ions into PCM-C was also estimated. This parameter has a migratory nature and is determined by applying an alternating electric field with an amplitude of 10 mV to the investigated system. The diffusion impedance can be represented as the Warburg impedance Z_w as the sum of identical frequency-independent real and imaginary components of resistance, the phase shift between which is close to 45° [15]:

$$Z_W(j\omega) = \sigma(j\omega)^{-0.5} = \sigma\omega^{-0.5}(1-j), \qquad (3)$$

where σ is the Warburg coefficient, ω is the cyclic frequency, and j is an imaginary unit.

The electrochemical insertion process is described in terms of semi-infinite diffusion in the low frequency range. Under these conditions, the diffusion coefficient D of lithium ions can be calculated from the equation

$$\sigma = \frac{R\,T}{n^2\,F^2\,A\,c_{Li}\sqrt{2D}}, \qquad (4)$$

where R is the universal gas constant; T is the absolute temperature; n is the number of transferred electrons; F is the Faraday constant; A is the geometric area of the electrode; c_{Li} is the molar concentration of lithium ions transferred through the electrolyte and inserted into the volume of the electrode material or located on its surface.

The value of the Warburg coefficient σ was calculated from the slope of the linear part of the dependence $Z' = f(\omega^{-0.5})$ (Fig. 5).

As follows from Fig. 5, when $x < 0.078$ the low-frequency branch of the dependence $Z' = f(\omega^{-0.5})$ contains two linear sections, which indicates the existence of two kinetic processes characterized by different time constants. These processes are the electrodiffusion transfer of lithium ions in the PMC particles, on the surface of which the SEI film has not yet formed, and a similar process occurring in the film itself. It is quite obvious that these processes will be characterized by different diffusion coefficients. When $x = 0.078$, only one linear section is observed on the dependence $Z' = f(\omega^{-0.5})$ at low frequencies, which indicates the coverage of the entire PCM surface with the SEI film. The form of this dependence does not change significantly when the insertion degree x increases. Only the angle of inclination of the straight section to the axis $\omega^{-0.5}$ changes, which causes a change in the Warburg coefficient σ and, in turn, the diffusion coefficient D.

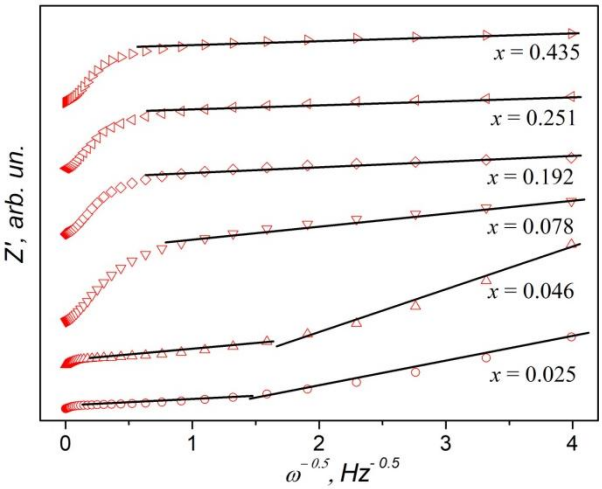

Fig. 5. Dependences $Z' = f(\omega^{-0.5})$ for PCM-C at different values x.

Analysis of the dependence $D = f(x)$ (Fig. 6) indicates a monotonic decrease in the diffusion coefficient with increasing of insertion degree x both at the initial stage of the process ($0.025 < x < 0.078$), when there are areas on the PCM surface free from the SEI film ($D_1 = 2\cdot10^{-8} \div 4\cdot10^{-11}$ cm²/s – curve 1), and areas covered by it ($D_2 = 1\cdot10^{-9} \div 1\cdot10^{-11}$ cm²/s – curve 2), and at $x \geq 0.078$, when the PCM surface is completely covered with a passivation film, the geometric sizes of which also increase with increasing x ($D_3 = 2\cdot10^{-11} \div 6\cdot10^{-12}$ cm²/s – curve 3).

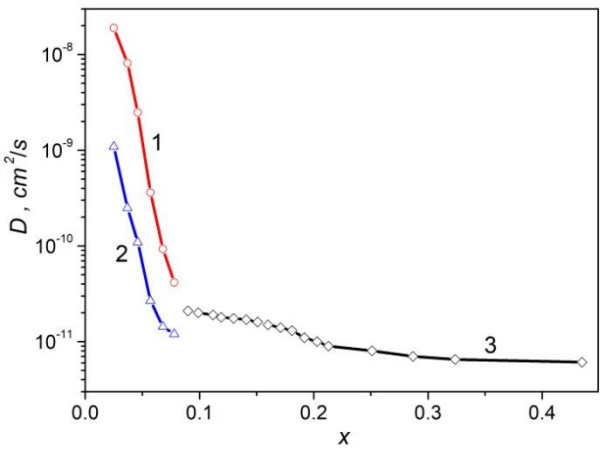

Fig. 6. Dependence of the diffusion coefficient of lithium ions on the x value when they are inserted into PCM-C (1), SEI film (2) and into the SEI / PCM-C structure (3).

It should be noted that the parameter D_3 is an averaged value that represents the processes of electrically stimulated diffusion of lithium ions both in the SEI film and in PCM-C. A sharp decrease of magnitude in the values of D_1 and D_2 by 2 - 3 orders at the initial stage of the electrochemical process corresponds to the formation of a near-surface layer in PCM-C enriched with inserted lithium ions, the electrostatic interaction of which complicates the process of further insertion. A slight

decrease in the parameter D_3, which is displayed by curve 3 in Fig. 6, indicates the stabilization of the process of electrochemical insertion of lithium ions into the electrode material PCM-C.

For the thermally activated material PCM-TA, a qualitative analysis of the Nyquist diagrams made it possible to find out that this process also has a staged nature (Fig. 7). In particular, the process of lithium ion insertion into this material is accompanied by the reduction of functional groups and the SEI formation on carbon particles at $0 < x < 0.187$. When $x \sim 0.187$, the PCM surface is completely covered with a passivation film, and with a further increase in the insertion degree x, this film grows in thickness and the formation of Li_xC phases occurs.

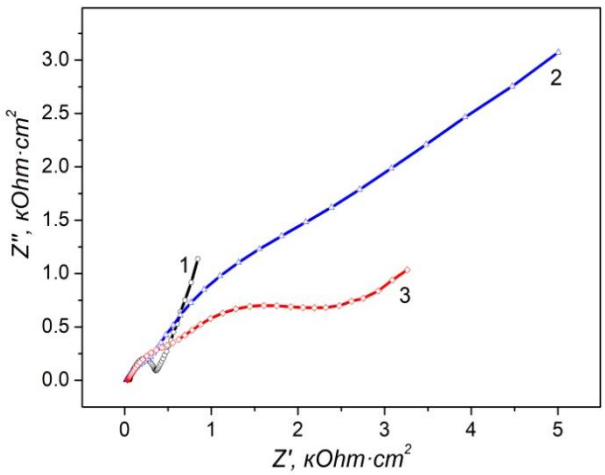

Fig. 7. Nyquist diagrams of an electrochemical system based on thermally activated PCM:
1 – $x = 0.019$; 2 – $x = 0.187$; 3 – $x = 0.229$.

Compared with the initial PCM-C sample (Fig. 1), the values of real and imaginary resistances for the electrochemical system based on the PCM-TA one (Fig. 7) are significantly lower for all values of the insertion degree x. The reason for this is the decrease in the surface fractal dimension $D_s = 2.34$ of the thermally activated material versus $D_s = 2.55$ for the PCM-C sample, the increase in the number of transport mesopores and their specific surface area from 51 m^2/g (for PCM-C) to 110 m^2/g (for PCM-TA) and the decrease in the proportion of micropores from 86% (for PCM-C) to 82% (for PCM-TA), despite the fact that the total specific surface area of the thermally activated material increased by 1.8 times (343 m^2/g for PCM-C and 614 m^2/g for PCM-TA) [18, 19].

For the proposed electrochemical processes, an EEC was selected that satisfactorily describes the electron-ion processes in the investigated system (Fig. 8). Although this scheme is the same in appearance for all values x, the physical content of its elements differs. In particular, the element R_{el} is the electrolyte resistance, the $CPE_1 \parallel R_1$ link describes the diffusion process of charge transfer across the electrolyte-SEI interface (the value of the parameter $CPE_{1P} = 0.62 \div 0.48$ when $0.019 < x < 0.187$), the $CPE_2 \parallel R_2$ link characterizes the charge accumulation at the electrolyte-PCM interface ($CPE_{2P} = 0.94 \div 0.83$ at the same values x). For these values x, the parameter CPE_3 has the physical content of inhomogeneous intercalation capacitance ($CPE_{3P} = 0.84 \div 0.76$).

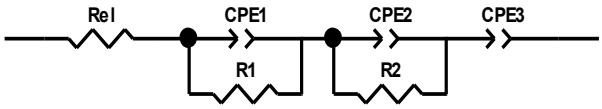

Fig. 8. EEC of process of lithium ion insertion into the PCM-TA sample.

At $x > 0.187$, when the sample surface is completely covered with SEI film, the physical content of the EEC parameters changes. In particular, the element CPE_1 has the physical content of the non-uniformly distributed DEL capacitance, which is formed on the SEI surface ($CPE_{1P} = 0.83 \div 0.94$). At the final stage of the process, the CPE_{1P} value is close to 1, which indicates the formation of an almost smooth (non-fractal) SEI film. The element CPE_2 changes from capacitive to diffusion ($CPE_{2P} = 0.79 \div 0.65$) when x increases, that indicates the dominance of diffusion processes, which are caused by the influx of lithium ions through the SEI film into the PCM-TA structure and the subsequent formation of Li_xC phases. The R_1 and R_2 elements have the physical content of the resistances of the corresponding processes. The parameter CPE_3 becomes the inhomogeneous Warburg diffusion impedance ($CPE_{3P} = 0.53 \div 0.46$).

The values of the parameters of the elements responsible for the process of SEI formation on carbon particles monotonically increase due to the growth of the SEI film (Fig. 9, a). As a result, diffusion restrictions are created on the penetration of lithium ions into the PCM-TA and the resistance of this film increases as a result of an increase in its thickness. A decrease in the contact area of the electrolyte with carbon, in turn, leads to a decrease in the DEL capacity, which is described by the element CPE_2, and the parameter R_2 increases several times due to the increase in the electrostatic repulsion between the inserted lithium ions (Fig. 9, b). The behavior of the element CPE_3 (Fig. 9, c) is the same as for the initial PCM-C (Fig. 3, c).

When x increases, there is a slight increase in the parameter CPE_1 (Fig. 10, a), which is probably due to the total contribution of the process of SEI formation in micro- and mesopores. The resistance of this layer increases sharply to 0.2 kOм·cm^2 (due to a further increase in its thickness), then decreases 0.135 kOм·cm^2 (most probably due to its densification and reduction of defects) and remains unchanged until the completion of the introduction process, that indicates the stabilization of the structure and properties of the electrode material. The stabilization of electron-ion processes is also indicated by the dependences of other EEC parameters on x, in particular at $x > 0.4$, where they remain unchanged (Fig. 10, b, c).

It should be noted that the parameters of the EEC elements undergo the greatest changes (compared to the parameters describing the electrochemical processes of lithium ion insertion into the PCM-C sample), which describe the charge transfer in the volume of carbon particles, i.e. the charge transfer resistance and diffusion limitations decrease. This indicates that the formation

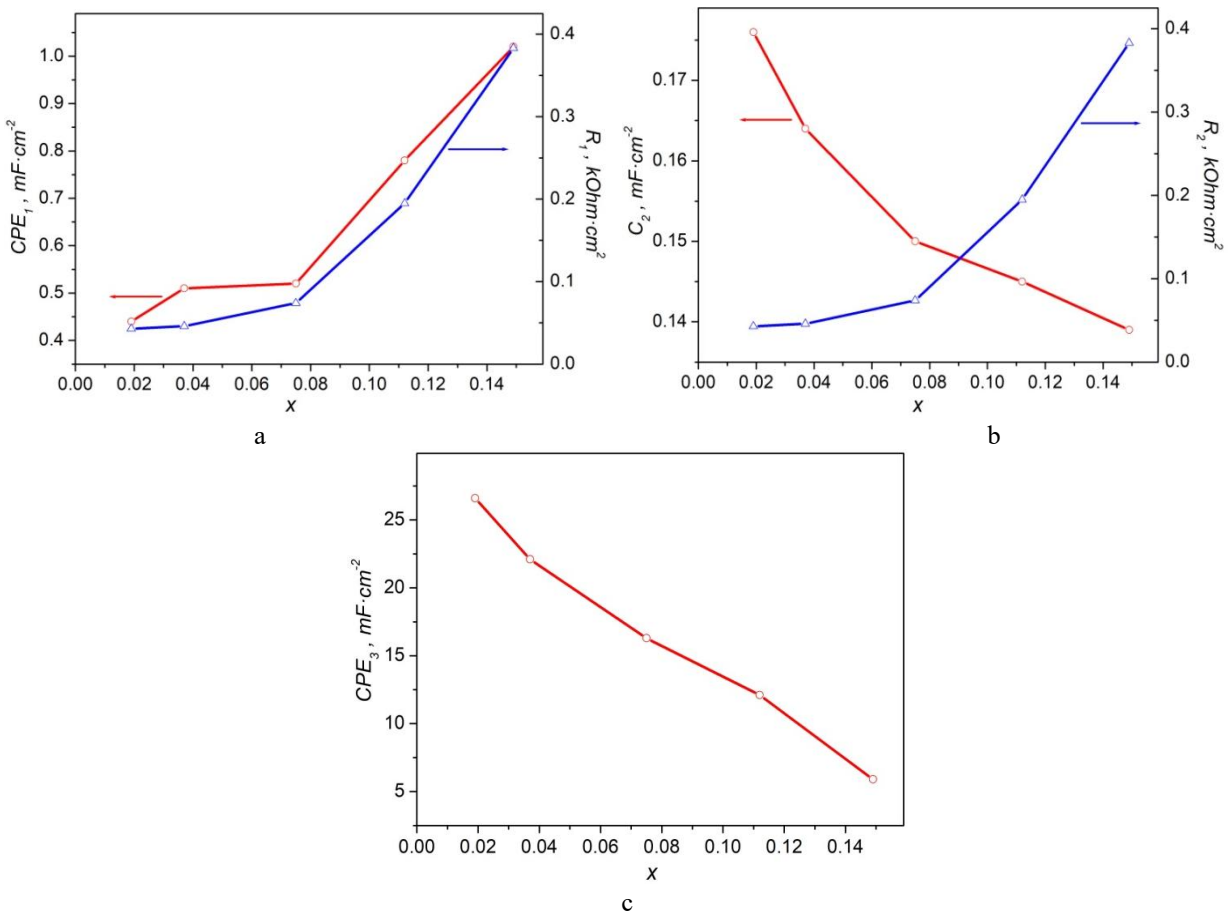

Fig. 9. Dependences of the EEC parameters on the insertion degree *x* at the first stage for PCM-TA sample.

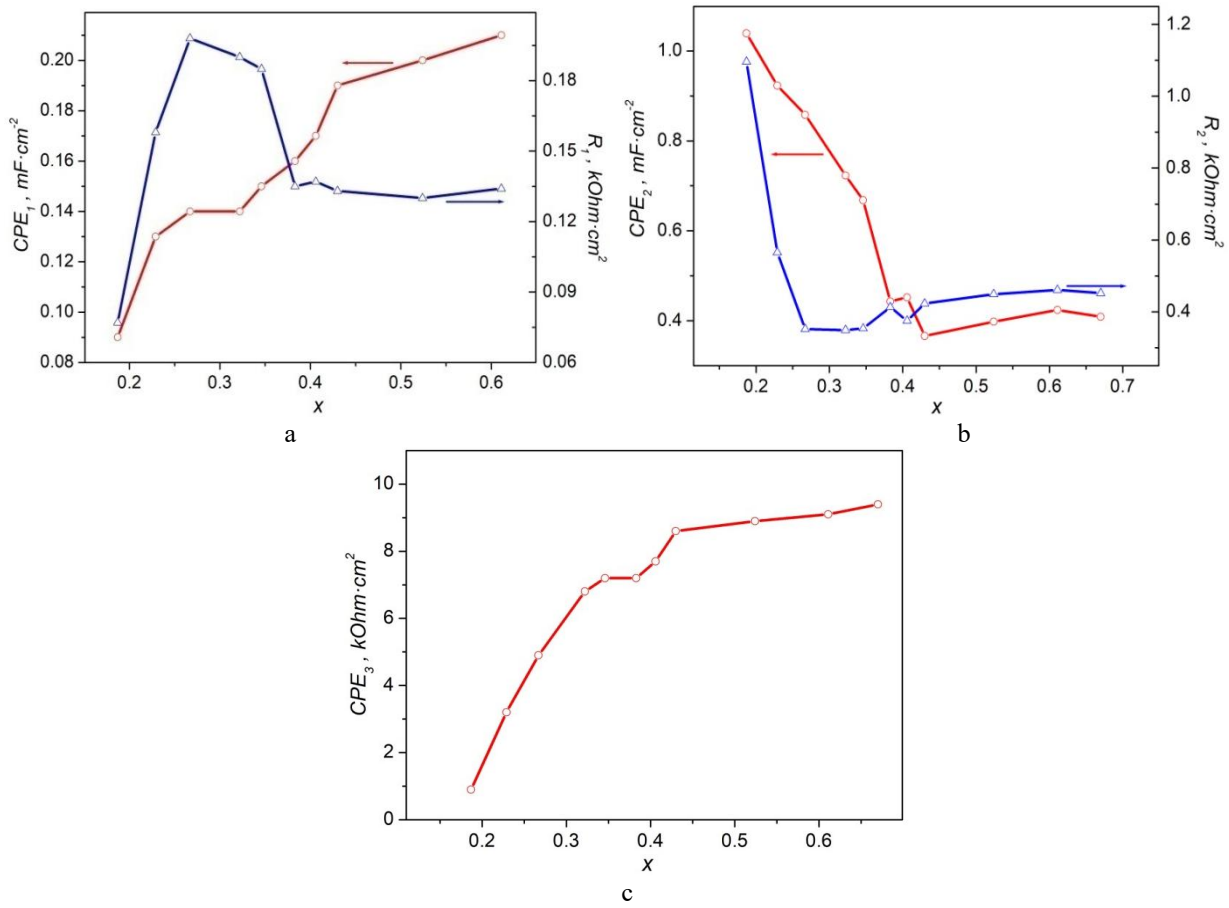

Fig. 10. Dependences of the EEC parameters on the insertion degreee at $x > 0.187$ for PCM-TA sample.

of a significant number of mesopores due to the opening of internal porosity during thermal activation of the initial sample, along with the formation of a more ideal SEI structure, creates more favorable kinetic conditions for the lithium ion insertion into the PCM-TA sample.

This conclusion is confirmed by the results of determining the diffusion coefficient of lithium ions D according to formula (4). For the PCM-TA sample, the diffusion coefficient decreases by 3 orders of magnitude ($D = 5\cdot10^{-8} \div 1\cdot10^{-11}$ cm^2/s) (Fig. 11), but it exceeds this value for the nitial sample by more than 2 times (Fig. 6). It should be noted that for the PCM-TA sample, when calculating the parameter D, it was not possible to clearly distinguish two linear sections at the initial stages of the lithium ion insertion on the dependences $Z' = f(\omega^{-0.5})$, which are used to calculate the Warburg coefficient σ, as it was in the case for the initial sample (Fig. 5). This result may indicate that thermal activation creates the preconditions for the formation of such states on the PCM surface, in which the localization of lithium ions is not energetically more favorable. As a result, the SEI film is formed simultaneously on the entire surface of the electrode material.

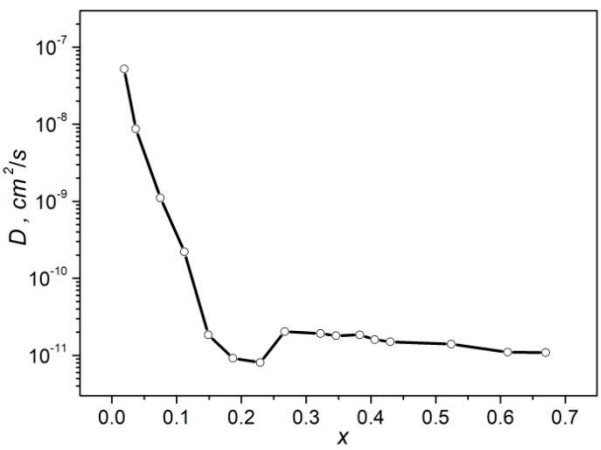

Fig. 11. Dependence of the diffusion coefficient of lithium ions on the value x for PCM-TA sample.

This character of the dependence $D = f(x)$ for weakly graphitized PCMs (Fig. 6 and 11) can be explained as the result of the simultaneous action of several factors: the interaction between the inserted lithium ions, the set of crystallographic positions for insertion and the dispersion of interplanar distances in the structure of the electrode material. Taking into account the fact that the investigated PCMs are characterized by a disordered structure in which the diffusion of lithium ions is difficult, it can be stated that the values D obtained in this work of the order of $10^{-7} \div 10^{-11}$ cm^2/s are reliable and do not contradict the literature data [20, 21].

Conclusions

It has been set that the process of electrochemical insertion of lithium ions into PCMs has a staged character, which consists in the formation of a solid electrolyte interface on carbon particles and the formation of non-stoichiometric insertion Li_xC phases.

For each of the indicated stages, equivalent electrical circuits were selected that satisfactorily model the impedance spectrum in the entire studied frequency range, and a physical interpretation was proposed for each circuit element. The dependences of the parameters of the equivalent electrical circuit on the insertion degree x were obtained and their behavior was analyzed.

Increasing the degree of lithium ion insertion for electrochemical systems based on both samples leads to an increase in the geometric dimensions of the solid electrolyte interface, as a result of which its resistance increases and the capacitance decreases. At the final stage of insertion, both parameters do not change noticeably, which indicates the stabilization of the structure and properties of this layer.

The opening of internal porosity, an increase in the proportion of mesopores, and the formation of a solid electrolyte interface more ideal in a structure create more favorable kinetic conditions for the lithium ion insertion into the PCM-TA sample, as a result of which the diffusion coefficient of lithium ions exceeds this value for the initial material more than 2 times and is $5\cdot10^{-8} \div 1\cdot10^{-11}$ cm^2/s when the insertion degree increases.

Mandzyuk V.I. – Doctor in Physics and Mathematics, Professor of Department of Computer Engineering and Electronics;
Nagirna N.I. – Candidate in Physics and Mathematics, Teacher of Physics and Special Disciplines;
Solomovskyi R.V. – PhD Student, Department of Computer Engineering and Electronics;
Ostapyshyn N.A. – Student of Department of Computer Engineering and Electronics.

[1] Y. Chen, Y. Liao, Y. Qing, Y. Ding, Y. Wu, L. Li, S. Luo, Y. Wu, *Recent advances in plant-derived porous carbon for lithium–sulfur batteries,* Journal of Energy Storage, 99(A), 113186 (2024); https://doi.org/10.1016/j.est.2024.113186.
[2] D. Feng, Y. Li, X. Qin, L. Zheng, B. Guo, W. Dai, N. Song, L. Liu, Y. Xu, Z. Tang, T. Gao *Biomass derived porous carbon anode materials for lithium-ion batteries with high electrochemical performance*, International Journal of Electrochemical Science, 19(3), 100488 (2024); https://doi.org/10.1016/j.ijoes.2024.100488.
[3] K. Zhou, S. Wang, S. Zhang, F. Kang, B. Li *Investigating the increased-capacity mechanism of porous carbon materials in lithium-ion batteries*, Journal of Materials Chemistry A, 28, 14031 (2020); https://doi.org/10.1039/D0TA04054A.
[4] H. Qutaish, S.A. Han, Y. Rehman, K. Konstantinov, M.-S. Park, J.H. Kim Porous carbon architectures with different dimensionalities for lithium metal storage, Science and Technology of Advanced Materials, 23(1), 169 (2020); https://doi.org/10.1080/14686996.2022.2050297.

[5] J. Ruan, Y. Xie, Z. Ye, *Research progress on the application of biomass-based porous carbon materials in lithium battery electrode*, Highlights in Science, Engineering and Technology, 40, 219 (2023); https://doi.org/10.54097/hset.v40i.6631.

[6] S. Ruan, X. He, H. Huang, Y. Gan, Y. Xia, J. Zhang, W. Wan, C. Wang, C. Xia, W. Zhang, *Innovative approaches of porous carbon materials derived from energy waste and their electrochemical properties,* Energy Mater., 5, 500066 (2025); http://dx.doi.org/10.20517/energymater.2024.217.

[7] K. Persson, V.A. Sethuraman, L.J. Hardwick, Y. Hinuma, Y.S. Meng, A. Van der Ven, V. Srinivasan, R. Kostecki, G. Ceder Lithium diffusion in graphitic carbon, J. Phys. Chem. Lett., 1, 1176 (2010); https://doi.org/10.1021/jz100188d.

[8] Y.-K. Huang, J. Pettersson, L. Nyholm, *Diffusion-Controlled Lithium* Trapping in Graphite Composite Electrodes for Lithium-Ion Batteries, Adv. Energy Sustainability Res., 3, 2200042 (2022); https://doi.org/10.1002/aesr.202200042.

[9] T. Uchida, Y. Morikawa, H. Ikuta, M. Wakihara, *Chemical diffusion coefficient of lithium in carbon fiber*, J. Electrochem. Soc., 143(8), 2606 (1996); https://doi.org/10.1149/1.1837055.

[10] S.-J. Kinkelin, F. Röder, K. Vogel, M. Steimecke, M. Bron, *A fundamental study on cyclic voltammetry at porous carbon thin-film electrodes*, Electrochim. Acta, 488, 144183 (2024); https://doi.org/10.1016/j.electacta.2024.144183.

[11] J.H. Park, H. Yoon, Y. Cho, C.-Y. Yoo, *Investigation of lithium ion diffusion of graphite anode by the galvanostatic intermittent titration technigue*, Materials, 14(16), 4683 (2021); https://doi.org/10.3390/ma14164683.

[12] J. Inamoto, S. Komiyama, S. Uchida, A. Inoo, Y. Matsuo, *Insight into the origin of the rapid charging ability of graphene-like graphite as a lithium-ion battery anode material using electrochemical impedance spectroscopy*, J. Phys. Chem. C, 126(38), 16100 (2022); https://doi.org/10.1021/acs.jpcc.2c04780.

[13] V.I. Mandzyuk, N.I. Nagirna, R.P. Lisovskiy, B.I. Rachiy, Y.T. Solovko, R.I. Merena, *The effect of thermal treatment of porous carbon on specific energy characteristics of lithium power sources on its basis,* Visnyk of Lviv Polytechnic National University, Electronics, 708, 84 (2011).

[14] V.I. Mandzyuk, N.I. Nagirna, R.P. Lisovskyy, *Morphology and electrochemical properties of thermal modified nanoporous carbon as electrode of lithium power sources*, Journal of Nano- and Electronic Physics, 6(1), 01017 (2014).

[15] E. Barsoukov, J.R. Macdonald, Impedance spectroscopy: theory, experiment, and applications (John Wiley & Sons Inc., New Jersey, 2018).

[16] P. Wang, D. Yan, C. Wang, H. Ding, H. Dong, J. Wang, S. Wu, X. Cui, C. Li, D. Zhao, S. Li, *Study of the formation and evolution of solid electrolyte interface via in-situ electrochemical impedance spectroscopy,* Applied Surface Science, 596, 153572 (2022); https://doi.org/10.1016/j.apsusc.2022.153572.

[17] P.B.Balbuena, Y. Wang, Lithium-ion batteries: solid-electrolyte interphase (London, 2004).

[18] V.I. Mandzyuk, R.P. Lisovskiy, *Fractal structure of nanoporous carbon obtained by hydrothermal carbonization of plant raw materials*, Journal of Nano- and Electronic Physics, 14(5), 05027 (2022); https://doi.org/10.21272/jnep.14(5).05027.

[19] V.I. Mandzyuk, R.P. Lisovskiy, Yu.O. Kulyk, B.I. Rachiy, R.V. Solomovskyi, *The effect of thermal modification of turbostratic carbon on its fractal structure,* Physics and Chemistry of Solid State, 25(1), 51 (2024); https://doi.org/10.15330/pcss.25.1.51-56.

[20] C.A. Leon y Leon, L.R. Radovic, Chemistry and Physics of Carbon (New York, 1994).

[21] H. Guo, X. Li, X. Zhang, H. Wang, Z. Wang, W. Peng, *Diffusion coefficient of lithium in artificial graphite, mesocarbon microbeads, and disordered carbon*, New Carbon Materials, 22(1), 7 (2007); https://doi.org/10.1016/s1872-5805(07)60006-7.

В.І. Мандзюк[1], Н.І. Нагірна[2], Р.В. Соломовський[1], Н.А. Остапишин[1]

Імпедансна спектроскопія карбонізованих та термічно активованих пористих вуглецевих матеріалів

[1]Прикарпатський національний університет імені Василя Стефаника, Івано-Франківськ, Україна,
volodymyr.mandzyuk@pnu.edu.ua
[2]Окремий структурний підрозділ «Професійний коледж електронних приладів Івано-Франківського національного технічного університету нафти і газу», Івано-Франківськ, Україна

За допомогою методу імпедансної спектроскопії проведено порівняльний аналіз кінетики електрохімічного впровадження іонів літію в пористий вуглецевий матеріал, отриманий гідротермальною карбонізацією рослинної сировини за температури 750°C (зразок PCM-C), та його подальшої термічної активації за температури Було проведено витримку при температурі 400°C протягом 2,5 год (зразок PCM-TA). Для електрохімічних систем на основі цих матеріалів було підібрано еквівалентні електричні схеми, які задовільно моделюють спектри імпедансу в досліджуваному діапазоні частот 10^{-2} -10^{6} Гц. Для кожного елемента схеми було запропоновано фізичну інтерпретацію. Було розраховано коефіцієнт дифузії іонів літію в структуру електродних матеріалів.

Ключові слова: пористий вуглецевий матеріал, карбонізація, термічна активація, електрохімічне введення, імпедансна спектроскопія, еквівалентна електрична схема, коефіцієнт дифузії.